Aag-initiated base excision repair drives alkylation-induced retinal degeneration in mice

Lisiane B. Meira[a], Catherine A. Moroski-Erkul[a], Stephanie L. Green[a], Jennifer A. Calvo[a], Roderick T. Bronson[b], Dharini Shah[a], and Leona D. Samson[a,1]

[a]Department of Biological Engineering and Center for Environmental Health Sciences, Massachusetts Institute of Technology, Cambridge, MA 02139; and [b]Rodent Histopathology Laboratory, Harvard Medical School, Boston, MA 02115

Edited by Jeremy Nathans, Johns Hopkins University School of Medicine, Baltimore, MD, and approved December 5, 2008 (received for review July 19, 2008)

Vision loss affects >3 million Americans and many more people worldwide. Although predisposing genes have been identified their link to known environmental factors is unclear. In wild-type animals DNA alkylating agents induce photoreceptor apoptosis and severe retinal degeneration. Alkylation-induced retinal degeneration is totally suppressed in the absence of the DNA repair protein alkyladenine DNA glycosylase (Aag) in both differentiating and postmitotic retinas. Moreover, transgenic expression of Aag activity restores the alkylation sensitivity of photoreceptors in *Aag* null animals. *Aag* heterozygotes display an intermediate level of retinal degeneration, demonstrating haploinsufficiency and underscoring that *Aag* expression confers a dominant retinal degeneration phenotype.

alkylation damage | DNA glycosylase | photoreceptors | apoptosis

Rods and cones are neuronal photoreceptor cells in the retina responsible for perception of light and color, respectively. Photoreceptor cell death via retinal degeneration leads to blindness and is a hallmark of a group of diseases collectively referred to as retinitis pigmentosa (RP) (1). Mutations in any of at least 45 different genes have been associated with RP, indicating a strong genetic component in retinal degeneration (www.sph.uth.tmc.edu/Retnet/sum-dis.htm). RP-associated retinal degeneration starts by rod cell death followed by cone loss, in a progressive process. Oxidative stress and oxidation-dependent DNA damage are thought to play a role in RP-associated photoreceptor apoptosis, and administration of antioxidants reduces cone cell death in the *rd1* mouse, a naturally-occurring mouse model of RP (2). Moreover, in experimental animals, excessive exposure to light (3) or exposure to the radiosensitizer nitroimidazole CI1010 (4, 5) induces retinal degeneration by mechanisms likely involving oxidative stress. Excessive light stimulates shedding of rod outer segments that are phagocytosed by retinal pigment epithelium (RPE) cells in a process that generates an excess of reactive oxygen and nitrogen species (RONS) (6, 7). That excessive light exposure ultimately induces DNA base damage has been inferred from the fact that such exposure induces increased expression of the DNA polymerase β (pol β) base excision repair (BER) enzyme (3). Moreover, a mouse model defective in transcription-coupled repair of oxidative DNA damage, the *Csb* mutant mouse, was recently reported to manifest retinal degeneration associated with aging or ionizing radiation exposure (8, 9), conditions where increased oxidative stress can occur.

Previous studies have shown that treatment with DNA alkylating agents leads to retinal degeneration in rodents (10–12). These studies were performed with the S_N1 alkylating agent methyl nitrosourea (MNU), which reacts with both oxygens and nitrogens in DNA to form 3 major adducts, 7-methylguanine (7MeG; 70–80% of all adducts), O^6-methylguanine (O^6MeG; ≈10%), and 3-methyladenine (3MeA; ≈10%). Increased levels of 7MeG, a lesion believed to be biologically inert, were detected in retinas of MNU-treated mice (13), but the question of which alkylated DNA lesions, if any, are responsible for inducing retinal degeneration has not been addressed. In other cell types, MNU's cytotoxicity has been largely attributed to O^6MeG lesions; unrepaired O^6MeGs mispair with thymine during replication and lead to cell death via apoptosis in a replication and DNA mismatch repair-dependent manner (14). Resistance to MNU-induced cytotoxicity is efficiently achieved via the direct repair of O^6MeG by the Mgmt DNA repair methyltransferase, a suicidal enzyme that transfers the methyl group from O^6MeG to its active-site cysteine residue, and is subsequently targeted for degradation (15). However, in addition to MNU-induced retinal degeneration being observed in animals treated in utero or as neonates when retinal cells are actively dividing (11, 16), degeneration was also observed in animals treated as adults (10, 12, 13), when retinal cells are quiescent and not actively dividing (17, 18). Thus, MNU-induced retinal cytotoxicity does not appear to be replication dependent and is therefore unlikely to be induced by O^6MeG.

Here, we report that treatment with methyl methanesulfonate (MMS), an S_N2 alkylating agent that produces almost negligible amounts of O^6MeG, leads to retinal degeneration in mice. We provide genetic evidence that alkylation-induced retinal degeneration depends on the action of the Aag DNA glycosylase, an enzyme that removes alkylated bases via cleavage of the glycosyl bond connecting the base to the sugar phosphate backbone, thus generating abasic sites that can be further processed by the BER machinery (19). Aag has a broad substrate specificity and in addition to recognizing and removing the alkylated bases 3MeA and 7MeG (major MMS-induced base lesions at ≈10% and ≈80%, respectively), it also recognizes 1,N^6-ethenoadenine, deaminated adenine (hypoxanthine, Hx), deaminated guanine (oxanine) (20–22), and 8oxoG (21), all of which are induced in response to RONS. We show that $Aag^{-/-}$ retinas are completely MMS-resistant. We provide definitive evidence that the Aag glycosylase drives alkylation-induced retinal cell death, and we show that Aag-induced cell death can occur independently of cell proliferation and that it does not involve O^6MeG. Moreover, we find that MMS-induced cell death is modulated by *Aag* gene copy number because $Aag^{+/-}$ have intermediate levels of alkylation-induced retinal degeneration. In addition, *Aag* cDNA transgenic mice are even more sensitive than wild type to alkylation-induced retinal degeneration. Our results indicate that Aag-dependent processing of alkylation damage is toxic to photoreceptors and shed light on the mechanisms of alkylation-induced retinal degeneration.

Author contributions: L.B.M. and L.D.S. designed research; L.B.M., C.A.M.-E., S.L.G., J.A.C., and D.S. performed research; L.B.M., C.A.M.-E., and R.T.B. analyzed data; and L.B.M. and L.D.S. wrote the paper.

The authors declare no conflict of interest.

This article is a PNAS Direct Submission.

Freely available online through the PNAS open access option.

[1]To whom correspondence should be addressed. E-mail: lsamson@mit.edu.

This article contains supporting information online at www.pnas.org/cgi/content/full/0807030106/DCSupplemental.

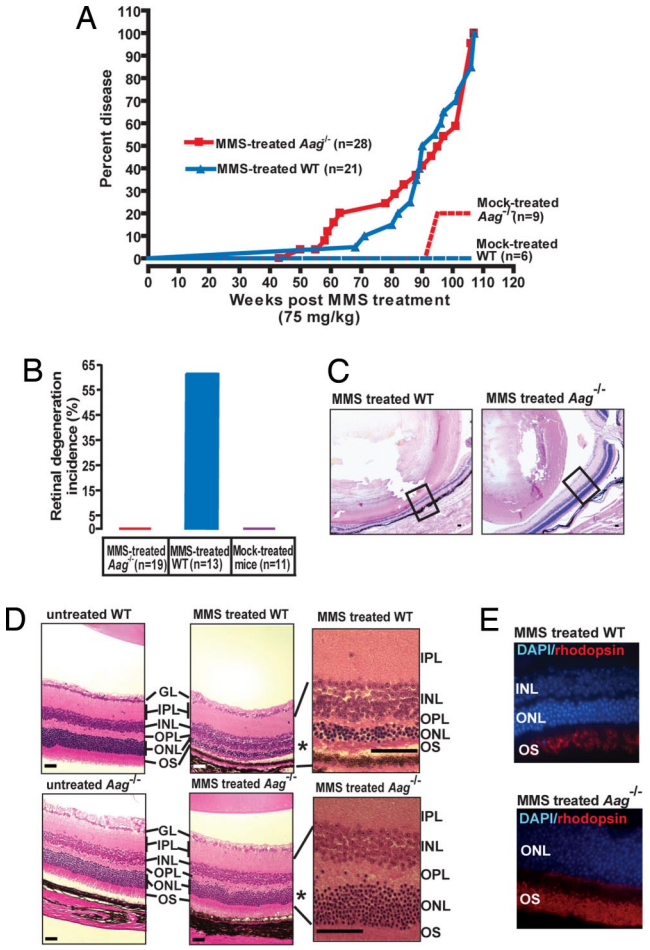

Fig. 1. *Aag*$^{-/-}$ animals are protected from MMS-induced retinal degeneration. (*A*) Kaplan-Meyer plot of survival for *Aag*$^{-/-}$ (n = 28) and wild-type animals (n = 21) treated with a single i.p. injection of 75 mg/kg MMS or mock-treated (wild type, n = 6; *Aag*$^{-/-}$, n = 9). (*B*) Increased incidence of retinal degeneration is seen only in wild-type-treated animals. Please note that good histological retinal samples were not obtained for all animals in the treated cohort, therefore the numbers of animals examined in *B* is lower than the total shown in *A*. (*C*) Photomicrograph comparing the striking retinal degeneration in a MMS-treated wild-type animal with the healthy retina seen in a MMS-treated *Aag*$^{-/-}$ animal. Box represents region in the retina that is shown magnified in *D*. (Magnification: 40×; bar: 1 mm.) (*D*) Photomicrographs depicting H&E-stained untreated retinas from adult wild-type and *Aag*$^{-/-}$ mice and retinas from MMS-treated wild-type and *Aag*$^{-/-}$ mice. (Magnification: 100×.) Region indicated by * is magnified 600× for detail. GL, ganglion cell layer; IPL, inner plexiform layer; INL, inner nuclear layer; OPL, outer plexiform layer; OS, outer segments. (*E*) Fluorescent staining of MMS-treated wild-type and *Aag*$^{-/-}$ retinas with DAPI (DNA stain = blue) and anti-rhodopsin antibody (rods = red). (Magnification: 600×.)

Results

Here, we demonstrate that Aag-initiated BER renders retinal photoreceptors sensitive to alkylation-induced cell death. A sublethal dose of the S_N2 alkylating agent MMS was administered to 8-day-old or 6- to 8-week-old wild-type and *Aag*$^{-/-}$ animals that were then observed over the next 2 years for long-term health assessment. Fig. 1*A* shows the survival for both genotypes; because survival latency was not significantly changed by age at time of MMS administration (data not shown), data for both age groups were combined. For both genotypes, MMS exposure significantly reduced disease-free lifespan, with *Aag*$^{-/-}$ animals succumbing to disease slightly sooner than wild-type animals (Fig. 1*A*). Although MMS induced a wide variety of tumor pathologies, the prevalence of which differed between wild type and *Aag*$^{-/-}$ (to be described elsewhere), the most striking difference between the 2 genotypes was the induction of retinal degeneration. Surprisingly, alkylation-induced retinal degeneration was only found in wild-type animals and not at all in *Aag*$^{-/-}$ animals. No mock-treated animal of either genotype displayed retinal degeneration (Fig. 1*B*). Fig. 1*C* shows the gross appearance of representative eyes of MMS-treated wild-type animals (*Left*) compared with MMS-treated *Aag*$^{-/-}$ animals (*Right*). The striking effect of MMS treatment in the wild-type retina is even more obvious in Fig. 1*D* that shows representative photomicrographs illustrating the extent of photoreceptor cell loss, represented by gross reduction in the outer nuclear layer (ONL) in wild type, and the lack of such a response in *Aag*$^{-/-}$ animals; the ONL contains the photoreceptor rods and cones. The reduction in the ONL from 11 to ≈2–5 cell layers in the treated wild type but not in *Aag*$^{-/-}$ indicates that the presence of Aag activity in the wild type drives degeneration (Fig. 1*D*). Staining with an antibody against the rod-specific protein rhodopsin demonstrates severe reduction in rod numbers, although the extent of cell loss in the ONL suggests that cones are also affected (Fig. 1*E*). TUNEL staining of wild-type and *Aag*$^{-/-}$ retinas confirms that the ONL is the affected retinal cell layer and that photoreceptors are dying via apoptosis (Fig. S1).

Among the cohort that was assessed long term after MMS treatment, retinal degeneration was seen in roughly similar proportions among wild-type animals treated at either the neonatal or the young adult stage (54% and 75%, respectively). Because 1–2 years had elapsed between MMS exposure and the time of death, it remained formally possible that the retinal degeneration observed in aged animals had been exacerbated by housing conditions, for instance by excessive light exposure. To address this possibility and confirm that MMS-induced retinal degeneration was initiated in both proliferating (neonatal) and quiescent (young adult) neurons, we treated neonates and young adult animals with MMS and monitored retinal degeneration in the days immediately after MMS exposure. For neonates, wild-type and *Aag*$^{-/-}$ postnatal day 7 (PND7) animals were treated with the same sublethal dose of MMS described above, and eyes were harvested at 1, 2, and 7 days after treatment. Fig. 2*A* shows that ONL reduction is quite apparent in the wild-type retina by 24 and 48 h post-MMS, and that by 7 days the wild-type ONL is severely reduced. In comparison, the retinas from treated *Aag*$^{-/-}$ animals have no visible signs of ONL reduction up to 7 days after MMS administration (Fig. 2*A*). This scenario was repeated for MMS-treated young adults (Fig. 2*B*). Seven days after treatment at 6–8 weeks of age, we saw severe reduction in the ONL in wild type, whereas the ONL in *Aag*$^{-/-}$ animals was totally intact (Fig. 2*B*). We infer that alkylation-induced Aag-mediated photoreceptor cell death is rapid and can be induced in both proliferating and quiescent postmitotic neurons within several days after exposure.

To quantify and better characterize alkylation-induced photoreceptor cell death, we used flow cytometry to analyze retinal cells harvested from the eyes of MMS-treated wild-type, *Aag*$^{+/-}$, or *Aag*$^{-/-}$ mice. Eyes were harvested at the time points indicated in Fig. 2*C*, and the dissociated retinal cells were TUNEL-labeled to monitor apoptosis; a summary of flow cytometric data obtained for at least 3 animals per genotype, per time point is shown in Fig. 2*C*. Retinas from untreated animals of all genotypes had a low percentage of apoptotic cells; at 24 h after MMS treatment, increased apoptosis was apparent in the wild-type and the *Aag*$^{+/-}$ heterozygous mutants, whereas the *Aag*$^{-/-}$ animals showed no increase above control levels. Forty-eight hours after MMS, wild-type retinas had the highest levels of apoptotic cells, whereas *Aag*$^{-/-}$ retinas remained at control levels. Importantly, *Aag*$^{+/-}$ heterozygous mutants showed intermediate levels of

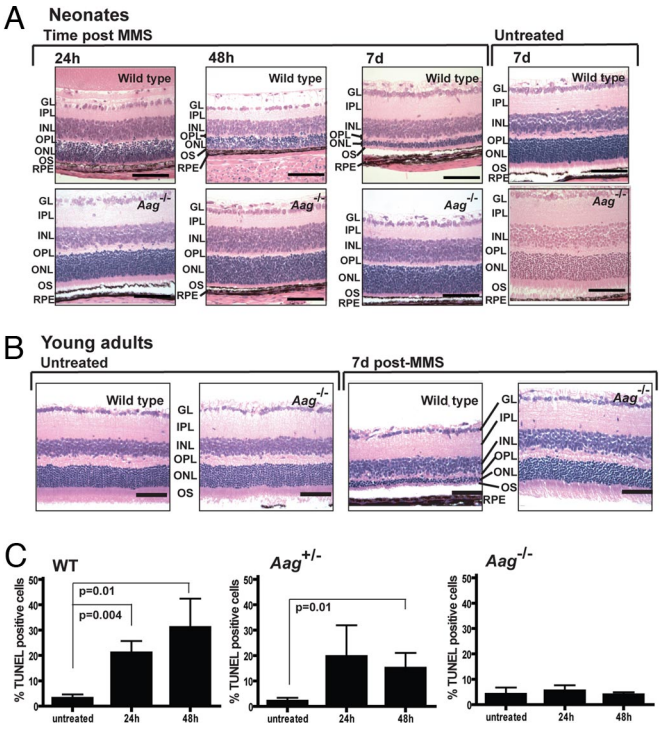

Fig. 2. Aag-dependent photoreceptor cell death occurs shortly after MMS treatment in both neonates and young adult wild-type animals. (*A*) Animals were treated at PND7. MMS-induced photoreceptor cell death was seen as early as 24 h after i.p. injection in a wild-type mouse, continued at 48 h after drug, and led to severe degeneration in the wild-type retina 7 days after treatment. $Aag^{-/-}$ animals are completely resistant to MMS, and 7 days after MMS administration there is no evidence of any photoreceptor cell loss in the retinas of $Aag^{-/-}$ animals. GL, ganglion cell layer; IPL, inner plexiform layer; INL, inner nuclear layer; OPL, outer plexiform layer; OS, outer segments. (Magnification: 400×; bar: 100 μm.) (*B*) Animals treated at 6–8 weeks of age with MMS. Representative photomicrographs are shown at a magnification of 400×. (Bars: 100 μm.) (*C*) Histogram graph representing quantification of MMS-induced retinal degeneration at the neonatal stage in at least 3 animals per time point. Apoptotic retinal cell death was quantified by flow cytometry in wild-type, $Aag^{+/-}$, and $Aag^{-/-}$ animals. Error bars represent SD.

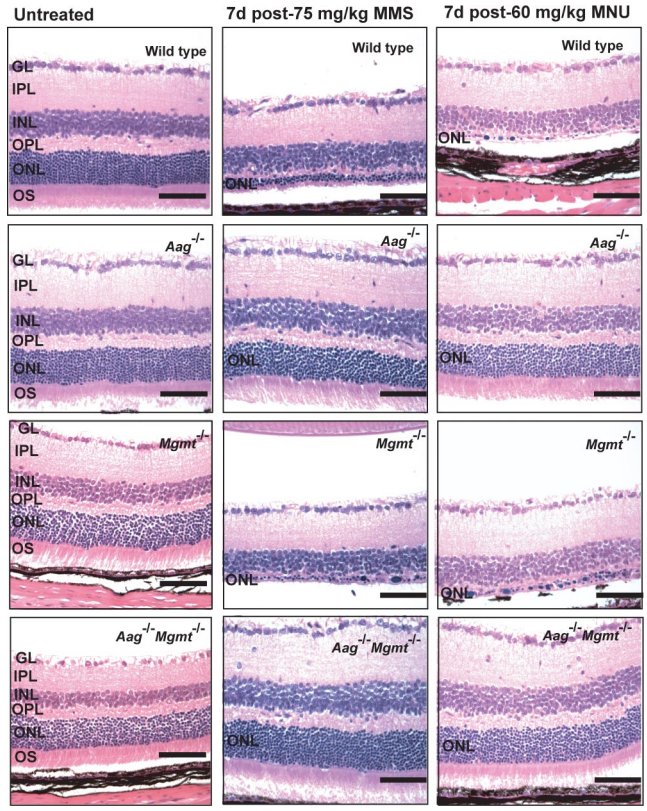

Fig. 3. Aag-dependent alkylation-induced retinal degeneration in mature retina. Animals of genotypes as shown were untreated (*Left*) or treated at 6–8 weeks of age with either 75 mg/kg MMS (*Center*) or 60 mg/kg MNU (*Right*). At least 3 animals were treated per genotype, per drug. GL, ganglion cell layer; IPL, inner plexiform layer; INL, inner nuclear layer; OPL, outer plexiform layer; OS, outer segments. Representative photomicrographs are shown at a magnification of 400×. (Bars: 100 μm.)

apoptosis, suggesting that Aag gene dosage plays an important role in modulating the extent of alkylation-induced apoptosis. The intermediate retinal degeneration phenotype in $Aag^{+/-}$ animals was also quite evident in stained tissue (data not shown).

As mentioned, the S_N1-alkylating agent MNU has also been shown to induce retinal degeneration in quiescent neurons in rats and hamsters (10, 12, 13). MNU, like MMS, induces 7MeG and 3MeA DNA lesions, both of which are Aag substrates, but in addition MNU induces a significant level of O^6MeG, an adduct that is not an Aag substrate. To determine whether O^6MeG might also play a role in alkylation-induced retinal degeneration, we examined O^6MeG repair-deficient $Mgmt^{-/-}$ mice for their sensitivity to alkylation-induced retinal degeneration. The results are shown in Fig. 3. Wild-type, $Aag^{-/-}$, $Mgmt^{-/-}$, and the $Aag^{-/-}$ $Mgmt^{-/-}$ double mutant young adult mice were treated with MNU and MMS (which induces very little O^6MeG). MMS and MNU induced retinal degeneration in wild-type mice, whereas $Aag^{-/-}$ mice were resistant to retinal degeneration induced by both MMS and MNU; $Mgmt^{-/-}$ animals were just as sensitive as wild-type animals to both MMS- and MNU-induced retinal degeneration (Fig. 3). Strikingly, the observed sensitivity in $Mgmt^{-/-}$ mice is completely suppressed by concomitant inactivation of the *Aag* gene (Fig. 3 *Bottom*). We infer that retinal degeneration induced by S_N1-alkylating agents does not involve O^6MeG. We also infer that alkylation-induced retinal degeneration completely depends on Aag activity and presumably on the excision of 3MeA and/or 7MeG DNA lesions. Aag-dependent excision of these base lesions would generate apurinic/apyrimidinic (AP) sites as BER intermediates, and we went on to show that significantly more AP sites are generated in retinal DNA in MMS-treated Aag-positive versus Aag-negative cells. These results are shown in Fig. S2.

Finally, we generated a transgenic animal expressing the mouse *Aag* cDNA from a ubiquitous promoter to confirm that Aag activity is indeed driving the observed alkylation-induced retinal degeneration. We administered MMS to young adult $Aag^{-/-}$ animals and $Aag^{-/-}$ animals expressing the *Aag* cDNA transgene; their retinas were examined 7 days after exposure. Fig. 4*A* shows that transgenic expression of Aag in $Aag^{-/-}$ mice restores extreme sensitivity to alkylation-induced retinal degeneration. The transgene confers a ≈4-fold increase in Aag DNA glycosylase activity (compared with wild type) as measured by the ability of retinal cell-free extracts to excise the Aag substrate Hx from DNA (Fig. 4*B*); the activity of another glycosylase (uracil DNA glycosylase) was similar for the extracts from wild-type, $Aag^{-/-}$, and $Aag^{-/-}$ mice expressing the transgene, confirming the integrity of the extracts (data not shown). Wild-type retina had relatively low Aag glycosylase activity but considerably more than the $Aag^{-/-}$ retina (Fig. 4*B*). Surprisingly, the relatively low glycosylase activity in wild-type retinal cells is enough to induce the severe retinal degeneration seen in MMS-treated wild-type animals.

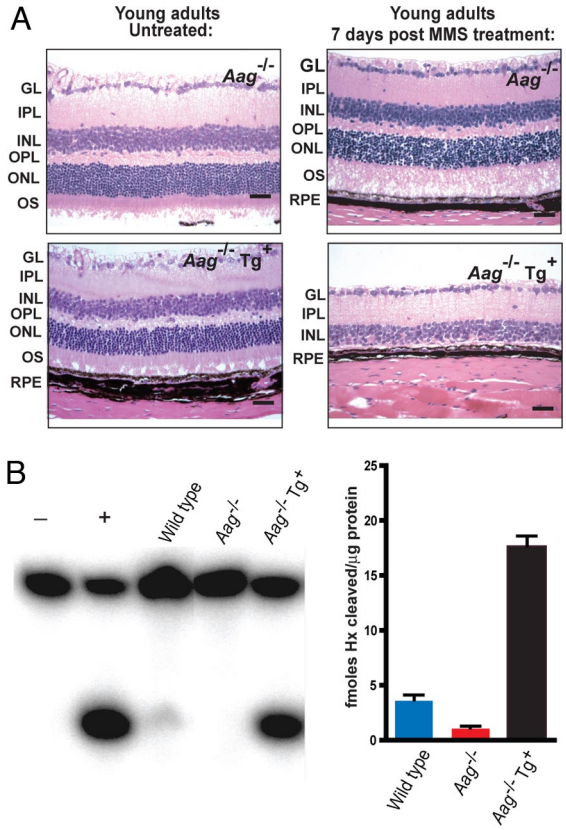

Fig. 4. Aag overexpression reverts the alkylation resistance of *Aag* mutant retinas. (*A*) Representative photomicrographs of retinas from $Aag^{-/-}$ mice or $Aag^{-/-}$ animals overexpressing the mouse Aag cDNA 7 days after treatment with 75 mg/kg of MMS. (Bars: 100 μm.) (*B*) (*Left*) Aag glycosylase activity on Hx–containing DNA on wild-type retinas, $Aag^{-/-}$ retinas, and retinas from $Aag^{-/-}$ animals overexpressing the mouse Aag cDNA ($Aag^{-/-}$ Tg^{+}). − represents no protein control, and + indicates reaction in the presence of purified human AAG protein. (*Right*) Histogram plots quantifying the amount of glycosylase activity for the gels shown in *Left*. Activity is expressed as fmol Hx per unit released per μg of protein. The Aag DNA glycosylase assays were performed as previously described (21). Error bars equal SD.

Discussion

Here, we describe the dramatic effects of a mild exposure to alkylating agents on the mouse retina, an exposure that leads to a moderate reduction in whole animal survival, but that has an acute effect on retinal degeneration. Wild-type mice treated with alkylating agents at both the neonatal and young adult stage display a profound loss of the retinal photoreceptor layer that is apparent within 1 week after treatment. We demonstrate that photoreceptor cell death entirely depends on the initiation of the BER pathway by the Aag DNA glycosylase. This conclusion is supported by the following: (*i*) Aag deficiency protects wild-type and $Mgmt^{-/-}$ animals from alkylation-induced photoreceptor cell death; (*ii*) Aag haploinsufficiency was evident because one functional Aag allele confers a level of alkylation-induced retinal degeneration that is intermediate between wild-type and null animals; and (*iii*) reintroduction of Aag activity into an $Aag^{-/-}$ animal (by transgene expression) totally suppresses the resistance of $Aag^{-/-}$ photoreceptors to alkylation-induced cytotoxicity.

Repair of DNA base damage occurs primarily by a multistep pathway wherein the sequential action of a number of enzymes ensures that a damaged base is removed, the resulting abasic site is cleaved, DNA ends are trimmed, correct nucleotides are inserted, and the remaining nicked DNA is ligated to restore the DNA to its native state (23). Modulation of the levels of individual BER enzymes leads to altered phenotypes in all model organisms tested so far (reviewed in ref. 24). Evidence from several laboratories indicates that BER imbalances are detrimental (25–30). We have shown in yeast that increased expression the Mag glycosylase (an Aag ortholog) leads to increased spontaneous mutagenesis (26) and that this phenotype is suppressed by coexpression of the Apn1 AP endonuclease that carries out the next step in the BER pathway (27). Increased expression of β-pol that acts subsequent to AP-endonuclease in the mammalian BER pathway, also leads to increased spontaneous mutagenesis in mammalian CHO cells (31), and evidence that tumor cell lines manifest increased β-pol expression has also been shown (32, 33). Imbalances in the BER pathway have the potential for allowing the accumulation of unrepaired DNA breaks and other BER intermediates that can lead to cell death and mutation. Indeed, we showed that inflamed colon tissue from ulcerative colitis patients has increased levels of AAG and the APE1 AP endonuclease (compared with uninflamed tissue), presumably induced to repair the DNA base damage that is inflicted by RONS during the inflammatory response. It turns out that such increased AAG and APE1 expression causes microsatellite instability (25).

Retinal degeneration induced by MNU has been reported (11–13). As an S_N1-alkylating agent, MNU generates the known toxic and mutagenic O^6MeG DNA lesion in addition to 3MeA and 7MeG. Here, we show that MMS, an S_N2 alkylator that generates negligible amounts of O^6MeG, also leads to photoreceptor apoptotic cell death in wild-type mice and that this phenotype is totally suppressed by inactivation of the Aag glycosylase. Moreover, we find that O^6MeG repair-deficient *Mgmt* mutant mice are equally sensitive to MMS- and MNU-induced retinal degeneration and that a mutation in the *Aag* gene suppresses retinal degeneration induced by both MMS and MNU, not only in wild-type but also in $Mgmt^{-/-}$ animals. Taken together, these results suggest that both S_N1 and S_N2 alkylation-induced photoreceptor cell death depends on the initiation of the BER pathway by the Aag DNA glycosylase presumably at 3MeA and/or 7MeG DNA lesions. By reintroducing a mouse Aag cDNA into an $Aag^{-/-}$ animal we unequivocally demonstrate that the retinal degeneration we see in animals treated with alkylating agents completely depends on Aag.

Aag-initiated BER leading to the generation of toxic BER intermediates was also the mechanism proposed to explain the unexpected MMS resistance seen in $Aag^{-/-}$ bone marrow cells (34). In support of this hypothesis we found that the MMS hypersensitivity of β-pol-deficient mouse embryonic fibroblasts (MEFs), that cannot efficiently complete BER, also depended on a functional Aag protein (35). Bone marrow cells and MEFs rapidly proliferate and would therefore be expected to be sensitive to unrepaired BER intermediates. We report here that both developing (proliferating) and mature (quiescent) mouse retinas are sensitive to apoptosis induced by alkylating agents and that in both cases sensitivity depends on Aag-mediated initiation of BER. We also find that in wild-type retinas the number of AP sites generated after MMS treatment is significantly higher than in the $Aag^{-/-}$ retina, confirming that Aag activity on alkylated DNA bases is generating BER intermediates or AP sites (Fig. S2). In addition, we show that *Atm* mutant retinas are at least partially protected from alkylation-induced retinal degeneration, strongly suggesting that the DNA damage response pathway orchestrated by the Atm kinase is involved in signaling the apoptotic events that follow MMS treatment in wild-type mice (Fig. S3). Taken together, these results support the notion that for some cell types unrepaired 3MeA and 7MeG DNA lesions are well tolerated and that alkylation cytotoxicity is largely driven by the generation of Aag-initiated BER intermediates. This idea is underscored by the *Aag* haploinsufficiency we observed in the retina; $Aag^{+/-}$ heterozygous retinal cells

experience less MMS-induced death than wild-type mice, but more than $Aag^{-/-}$ null mice.

Retinal degeneration is a major symptom of the complex genetic disease RP. At least 45 genes have been identified that when mutated increase susceptibility to RP, but these account for only about half of all RP patients (1). Thus far, the affected biochemical pathways leading to RP involve proteins responsible for cell signaling and phototransduction, vitamin A metabolism, cytoskeletal structure, protein trafficking and RNA splicing (1). DNA repair has now been directly linked to retinal degeneration in 2 different mouse models, namely radiation-exposed *Csb* null mice that are deficient in transcription-coupled nucleotide excision DNA repair and as described here for alkylation-exposed mice that are proficient in the initiation of BER. Whether or not DNA damage and repair are involved in human RP has not yet been addressed. Having said that, it is quite clear that cigarette smoke is an important risk factor for retinal degeneration and that oxidative damage has been linked to RP (2, 36). Environmental exposures can induce both DNA alkylation and oxidation (37), either directly or as a consequence of inducing an inflammatory response (38, 39). The mouse Aag and human AAG DNA repair glycosylases recognize and excise DNA base lesions produced by both alkylation and oxidation damage to the cell. Given the profound role that this DNA repair enzyme plays in the mouse model, we propose that it may be an important player in the development of environmentally-induced human retinal degenerative diseases in both children and adults.

Methods

Mice. The $Aag^{-/-}$ mice, now backcrossed for >12 generations onto a C57BL/6J background, have been described (21, 34). $Mgmt^{-/-}$ mice (described in ref. 40) and *Aag Mgmt* double mutant (this study) were also on a C57BL/6J background. Transgenic animals overexpressing the mouse *Aag* gene were generated by conventional pronuclear injection of a transgene consisting of the mouse *Aag* cDNA under the control of a promoter that is composed of an enhancer element from the CMV-immediate early promoter and the ubiquitous strong promoter derived from the chicken β-actin gene (41). Mice were fed a standard diet ad libitum and housed in an American Association for the Accreditation of Laboratory Animal Care-accredited facility. Animals were killed by CO_2 asphyxiation, and animal procedures were approved by the Massachusetts Institute of Technology Committee on Animal Care.

Reagents. MMS and MNU were obtained from Sigma–Aldrich. DAPI and the APO-BrdU TUNEL Assay kit were from Molecular Probes/Invitrogen. mAb against rhodopsin [RET-P1] was purchased from AbCam.

Experimental Treatments. ***MMS treatment for long-term health outcome.*** Wild-type and $Aag^{-/-}$ mice were treated with a single i.p. injection of MMS at a sublethal dose of 75 mg/kg in saline [this dose represents half of the LD_{50} dose for both wild-type and $Aag^{-/-}$ mice (34)]. Animals were treated as neonates at PND8 or as young adults at 6–8 weeks of age. Mock-treated animals were i.p.-injected with an equivalent volume of saline. Treated and mock-treated animals were allowed to age and observed for development of disease. Animals were subject to full necropsy when diseased or deceased or at 104 weeks after injection. Tissues were fixed in Bouin's fixative, paraffin-embedded, sectioned at 5 μm, and stained with H&E. Retinal degeneration diagnosis was assigned by the pathologist (R.T.B.) if severe reduction of photoreceptors in the ONL was seen, from the normal number of 11 cells per ONL to 5 or fewer cells per ONL.

Alkylation treatments for short-term retinal analysis. Wild-type and $Aag^{-/-}$ animals, at PND7 and 6–8 weeks of age were i.p.-injected with MMS (75 mg/kg) or MNU (60 mg/kg) and killed at different time points after injection. Eyes were removed and retinas were dissected with the help of a stereomicroscope. Retinas were fixed in 10% neutral buffered formalin overnight, embedded in paraffin, sectioned at 5 μm, and H&E-stained for histopathological analysis.

FACS Analysis. Wild-type, $Aag^{+/-}$, and $Aag^{-/-}$ animals were i.p.-injected with MMS (75 mg/kg) at 4 days of age, and retinas were harvested 24 and 48 h after treatment. Dissected retinas were incubated in trypsin for cell dissociation. Cells were fixed in 3.7% formalin for 1 min and then methanol for 1 min. Fixed cells were TUNEL-labeled by using the Apo-BrdU TUNEL Assay kit (Invitrogen) following the manufacturer's directions. Total amount of retinal cells was analyzed by FACS with gating performed to eliminate cellular debris and larger cell aggregates (by side and forward scattering). At least 3 animals were used for each treatment, and time point and at least 10,000 cells per events were analyzed per experimental point. GraphPad Prism software was used for statistical analyses. The Mann–Whitney test was used to compare apoptosis levels in the different time points.

Immunofluorescence Analysis. Retinas (5-μm-thick sections) were deparaffinized and rehydrated in a graded ethanol series, incubated in citrate buffer, and thermally processed in a benchtop Retriever (PickCell Labs). Sections were blocked in 10% goat serum for 10 min and labeled with anti-rhodopsin (1/400 dilution) for 30 min. After 3 washes in PBS-T, sections were incubated for 30 min with a 1/400 dilution of the secondary antibody Alexa594 (Molecular Probes/Invitrogen) in the dark. Slides were counterstained with DAPI (1/200) and then observed with a Nikon Eclipse E800 fluorescence microscope equipped with a Retiga EXi Fast 1394 CCD camera. Image acquisition and analysis was done with Volocity software (Improvision).

In Vitro Alkyladenine DNA Glycosylase Assay. Cell extracts were made from mouse retinas that were wild-type, $Aag^{-/-}$, and $Aag^{-/-}$ Tg^{+} in glycosylase assay buffer [20 mM Tris·Cl (pH 7.6), 100 mM KCl, 5 mM EDTA, 1 mM EGTA, and 5 mM β-mercaptoethanol] along with protease inhibitors, followed by sonication. Protein concentration was measured with a micro BCA Kit (Pierce).

See *SI Text* for additional details on methods.

ACKNOWLEDGMENTS. We thank Kristin Glavine and Dawn P. Spelke for help in the initial stages of this project; and Alicia Caron and Glen Paradis (MIT, Cambridge, MA) for their help with histology and flow cytometry, respectively. L.D.S. is an American Cancer Society Research Professor. This work was supported by National Institutes of Health Grants ES02109, CA55042, and CA75576.

1. Hartong DT, Berson EL, Dryja TP (2006) Retinitis pigmentosa. *Lancet* 368:1795–1809.
2. Komeima K, Rogers BS, Lu L, Campochiaro PA (2006) Antioxidants reduce cone cell death in a model of retinitis pigmentosa. *Proc Natl Acad Sci USA* 103:11300–11305.
3. Gordon WC, Casey DM, Lukiw WJ, Bazan NG (2002) DNA damage and repair in light-induced photoreceptor degeneration. *Invest Ophthalmol Visual Sci* 43:3511–3521.
4. Miller TJ, *et al.* (2006) Photoreceptor cell apoptosis induced by the 2-nitroimidazole radiosensitizer, CI-1010, is mediated by p53-linked activation of caspase-3. *Neurotoxicology* 27:44–59.
5. Miller TJ, Phelka AD, Tjalkens RB, Dethloff LA, Philbert MA (2003) CI-1010 induced opening of the mitochondrial permeability transition pore precedes oxidative stress and apoptosis in SY5Y neuroblastoma cells. *Brain Res* 963:43–56.
6. Miceli MV, Liles MR, Newsome DA (1994) Evaluation of oxidative processes in human pigment epithelial cells associated with retinal outer segment phagocytosis. *Exp Cell Res* 214:242–249.
7. Tate DJ, Jr, Miceli MV, Newsome DA (1995) Phagocytosis and H2O2 induce catalase and metallothionein gene expression in human retinal pigment epithelial cells. *Invest Ophthalmol Visual Sci* 36:1271–1279.
8. van der Pluijm I, *et al.* (2006) Impaired genome maintenance suppresses the growth hormone–insulin-like growth factor 1 axis in mice with Cockayne syndrome. *PLoS Biol* 5:e2.
9. Gorgels TG, *et al.* (2007) Retinal degeneration and ionizing radiation hypersensitivity in a mouse model for Cockayne syndrome. *Mol Cell Biol* 27:1433–1441.
10. Nakajima M, *et al.* (1996) Photoreceptor apoptosis induced by a single systemic administration of *N*-methyl-*N*-nitrosourea in the rat retina. *Am J Pathol* 148:631–641.
11. Taomoto M, *et al.* (1998) Retinal degeneration induced by *N*-methyl-*N*-nitrosourea in Syrian golden hamsters. *Graefes Arch Clin Exp Ophthalmol* 236:688–695.
12. Yuge K, *et al.* (1996) *N*-methyl-*N*-nitrosourea-induced photoreceptor apoptosis in the mouse retina. *In Vivo* 10:483–488.
13. Ogino H, *et al.* (1993) Retinal degeneration induced by *N*-methyl-*N*-nitrosourea and detection of 7-methyldeoxyguanosine in the rat retina. *Toxicol Pathol* 21:21–25.
14. Hickman MJ, Samson LD (1999) Role of DNA mismatch repair and p53 in signaling induction of apoptosis by alkylating agents. *Proc Natl Acad Sci USA* 96:10764–10769.
15. Srivenugopal KS, Yuan XH, Friedman HS, Ali-Osman F (1996) Ubiquitination-dependent proteolysis of O6-methylguanine-DNA methyltransferase in human and murine tumor cells after inactivation with O6-benzylguanine or 1,3-bis(2-chloroethyl)-1-nitrosourea. *Biochemistry* 35:1328–1334.
16. Smith SB, Yielding KL (1986) Retinal degeneration in the mouse. A model induced transplacentally by methylnitrosourea. *Exp Eye Res* 43:791–801.
17. Reh TA, Levine EM (1998) Multipotential stem cells and progenitors in the vertebrate retina. *J Neurobiol* 36:206–220.
18. Cepko CL, Austin CP, Yang X, Alexiades M, Ezzeddine D (1996) Cell fate determination in the vertebrate retina. *Proc Natl Acad Sci USA* 93:589–595.
19. Wyatt MD, Allan JM, Lau AY, Ellenberger TE, Samson LD (1999) 3-Methyladenine DNA glycosylases: Structure, function, and biological importance. *BioEssays* 21:668–676.

20. Hitchcock TM, *et al.* (2004) Oxanine DNA glycosylase activity from mammalian Alkyl-Adenine glycosylase. *J Biol Chem* 279:38177–38183.
21. Engelward BP, *et al.* (1997) Base excision repair deficient mice lacking the Aag alkyladenine DNA glycosylase. *Proc Natl Acad Sci USA* 94:13087–13092.
22. Ham AJ, *et al.* (2004) New immunoaffinity-LC-MS/MS methodology reveals that Aag null mice are deficient in their ability to clear 1,N6-etheno-deoxyadenosine DNA lesions from lung and liver in vivo. *DNA Repair (Amst)* 3:257–265.
23. Wyatt MD, Pittman DL (2006) Methylating agents and DNA repair responses: Methylated bases and sources of strand breaks. *Chem Res Toxicol* 19:1580–1594.
24. Larsen E, Meza TJ, Kleppa L, Klungland A (2007) Organ and cell specificity of base excision repair mutants in mice. *Mutat Res* 614:56–68.
25. Hofseth LJ, *et al.* (2003) The adaptive imbalance in base excision-repair enzymes generates microsatellite instability in chronic inflammation. *J Clin Invest* 112:1887–1894.
26. Xiao W, Samson L (1993) In vivo evidence for endogenous DNA alkylation damage as a source of spontaneous mutation in eukaryotic cells. *Proc Natl Acad Sci USA* 90:2117–2121.
27. Glassner BJ, Rasmussen LJ, Najarian MT, Posnick LM, Samson LD (1998) Generation of a strong mutator phenotype in yeast by imbalanced base excision repair. *Proc Natl Acad Sci USA* 95:9997–10002.
28. Sobol RW, *et al.* (2003) Base excision repair intermediates induce p53-independent cytotoxic and genotoxic responses. *J Biol Chem* 278:39951–39959.
29. Bergoglio V, *et al.* (2002) Deregulated DNA polymerase beta induces chromosome instability and tumorigenesis. *Cancer Res* 62:3511–3514.
30. Zhang H, *et al.* (2007) Targeting human 8-oxoguanine DNA glycosylase (hOGG1) to mitochondria enhances cisplatin cytotoxicity in hepatoma cells. *Carcinogenesis* 28:1629–1637.
31. Canitrot Y, *et al.* (1998) Overexpression of DNA polymerase β in cell results in a mutator phenotype and a decreased sensitivity to anticancer drugs. *Proc Natl Acad Sci USA* 95:12586–12590.
32. Canitrot Y, *et al.* (2006) Enhanced expression and activity of DNA polymerase β in chronic myelogenous leukemia. *Anticancer Res* 26:523–525.
33. Bergoglio V, *et al.* (2001) Enhanced expression and activity of DNA polymerase β in human ovarian tumor cells: Impact on sensitivity toward antitumor agents. *Oncogene* 20:6181–6187.
34. Roth RB, Samson LD (2002) 3-Methyladenine DNA glycosylase-deficient Aag null mice display unexpected bone marrow alkylation resistance. *Cancer Res* 62:656–660.
35. Sobol RW, *et al.* (2002) Mutations associated with base excision repair deficiency and methylation-induced genotoxic stress. *Proc Natl Acad Sci USA* 99:6860–6865.
36. Carmody RJ, Cotter TG (2000) Oxidative stress induces caspase-independent retinal apoptosis in vitro. *Cell Death Differ* 7:282–291.
37. Hecht SS (1999) DNA adduct formation from tobacco-specific N-nitrosamines. *Mutat Res* 424:127–142.
38. Brody JS, Spira A (2006) State of the art: Chronic obstructive pulmonary disease, inflammation, and lung cancer. *Proc Am Thorac Soc* 3:535–537.
39. Meira LB, *et al.* (2008) DNA damage induced by chronic inflammation contributes to colon carcinogenesis. *J Clin Invest* 118:2516–2525.
40. Glassner BJ, *et al.* (1999) DNA repair methyltransferase (*Mgmt*) knockout mice are sensitive to the lethal effects of chemotherapeutic alkylating agents. *Mutagenesis* 14:339–347.
41. Niwa H, Yamamura K, Miyazaki J (1991) Efficient selection for high-expression transfectants with a novel eukaryotic vector. *Gene* 108:193–199.